25th ABCM International Congress of Mechanical Engineering
October 20-25, 2019, Uberlândia, MG, Brazil

COB-2019-2297
STABILIZED FINITE ELEMENT APPROXIMATIONS FOR SHEAR-THINNING VISCOELASTIC FLOWS

Natan A. Oliveira
Vitor dal B. Abella
Sérgio L. Frey
Laboratory of Applied and Computational Mechanics – LAMAC, Universidade Federal do Rio Grande do Sul – UFRGS, Sarmento Leite, 425 Porto Alegre, RS/Brazil — 90050-170
natan.oliveira@mecanica.ufrgs.br
vitor.abella@mecanica.ufrgs.br
frey@mecanica.ufrgs.br

Abstract. *Viscoelastic fluids are present in several industrial applications in nature. The current work aims at investigating viscoelastic flows in complex flows, in particular through a sudden contraction with a variable aspect ratio. The mechanical model is made-up of conservation equations of mass and momentum for incompressible materials, coupled with a modified upper convected Maxwell–type equation that accommodates the shear-thinning of viscosity. The model is via a three-field Galerkin least-squares–like method in extra stress, velocity, and pressure. Computations focus on the evaluation of the influence of elasticity, kinematics, power-law, and geometry. That is obtained by the ranging in inappropriate intervals, of the Weissenberg number, the flow rate, the power coefficient, and the aspect ration of the contraction. Numerical results make clear that elasticity and geometry alter the viscoelastic flow pattern profoundly.*

Keywords: *viscoelastic, White-Metzner equation, shear-thinning, stabilized finite element, sudden contraction*

1. INTRODUCTION

Most industrial fluids do not follow Newton's viscosity law established in the 17th century. For these fluids, the relationship between the applied stress and the mechanical response obtained ceases to be constant for being a function of flow deformation. Many of them still exhibit a more complex behavior as memory, non-zero first normal stress difference and dependence of time. Among the so-called complex fluids stand out the viscoelastic, elasto-viscoplastic thixotropic materials. Some examples of this class of materials – called non-Newtonian – are paints, cosmetic products, foodstuff, and polymer extrusion.

A feasible numerical solution must be based upon physical and constitutive models that guarantee its physical meaning. Many constitutive models were proposed for modeling complex material with viscoelastic behavior. The widely used in numerical simulations is the upper-convected Maxwell (UCM) model. This major advance is the simple computational implementation while serious withdraw is the incapability to predict flows of polymeric solutions. Listing some works, we have the pioneering articles of Crochet and Bezy (1979) and Viriyayuthakorn and Caswell (1980). In the former, the authors implemented a three-field Galerkin formulation in pressure, extra-stress, and velocity. The element was applied to inertia flows of UCM viscoelastic materials, flowing through an axisymmetric sudden 2:1 contraction. In the latter, the authors implemented a mixed Galerkin element formulation using an integral quadrature formula. This new element as used to solve high-order UCM Stokes flows in axisymmetric sudden 4:1 contraction and expansion domains. In Cruz *et al.* (2014), the authors implemented a second-order finite volume method, coupled to log-conformation technique, to approximate Stokes flows of UCM, Oldroyd-B and simplified Phan-Thien–Tanner (SPTT) materials in a stationary bifurcation domain.

Listing more recent works, in Oliveira and Pinho (1999) the Authors implemented a finite volume method applied to the Navier-Stokes problem for UCM and SPTT materials flowing through a 4:1 axisymmetric sudden contraction. In Alves *et al.* (2004) the authors implemented the model proposed in Oliveira and Pinho (1999) for approximating viscoelastic inertialess flows in sudden contraction, subjected to various aspect ratio. In Tomé *et al.* (2008) the Authors also approximated viscoelastic inertialess flows in a 4:1 axisymmetric sudden contraction . In Frey *et al.* (2010) the Authors used a stabilized finite element method for approximating UCM viscoelastic materials flowing over a cylinder confined in a planar channel. In Cruz *et al.* (2014), the Authors implemented a second-order finite volume method, coupled with the log-conformation technique, for approximating Stokes flows of UCM, Oldroyd-B and simplified Phan-

Thien–Tanner (SPTT) materials in a stationary bifurcation domain.

This work performs numerical simulations of shear-thinning viscoelastic flows in a sudden contraction with a variable aspect ratio. The simulations are carried out via a three-field Galerkin least-squares–like method, in terms of extra stress, pressure, and velocity. The model makes use of the mass and momentum conservation equations – for constant-density materials – coupled with the White-Metzner (WM) to accommodate the shear-thinning of viscosity. Results aim at evaluating the sensibility of flow pattern to changes in kinematics, elasticity, geometry, and shear thinning. In this way, the dimensionless flow rate, number, and power-law index are respectively varied in wide and relevant ranges.

2. GOVERNING EQUATIONS

Assume a regular fluid domain $\Omega \subset \Re^2$ with polygonal boundaries Γ_g and Γ_h – the former subjected to Dirichlet conditions and the latter subjected to Neumann ones. Inertialess steady flows of a White-Metzner elastic material are governed by,

$$div\,\mathbf{u} = 0 \quad \text{in } \Omega \tag{1}$$

$$\mathbf{0} = -\nabla p + div\,\boldsymbol{\tau} + \rho\mathbf{f} \quad \text{in } \Omega \tag{2}$$

$$\boldsymbol{\tau} + \lambda\check{\boldsymbol{\tau}} = 2\eta(\dot{\gamma})\,\mathbf{D(u)} \quad \text{in } \Omega \tag{3}$$

where $\mathbf{u}$ is the velocity vector, $\boldsymbol{\tau}$ is the extra-stress tensor, p is the mean pressure, $\mathbf{f}$ is a given body force per mass unity, λ is the relaxation time, $\mathbf{D}(u)$ is the strain rate tensor, $\eta(\dot{\gamma})$ is the shear-thinning viscosity, and $\check{\boldsymbol{\tau}}$ is the upper-convected material derivative of the extra-stress tensor, for steady regimes.

$$\check{\boldsymbol{\tau}} = D_t\,\boldsymbol{\tau} - \boldsymbol{\tau}(\nabla\mathbf{u}) - (\nabla\mathbf{u})^T\boldsymbol{\tau} \tag{4}$$

with $D_t(\cdot)$ denoting the material derivative operator for steady flows reduced to, $D_t\,\boldsymbol{\tau} \equiv (\nabla\boldsymbol{\tau})\mathbf{u}$. The shear-thinning of viscosity, $\eta(\dot{\gamma})$, is the one introduced by Eq.(5),

$$\eta(\dot{\gamma}) = \eta_\infty + (\eta_0 - \eta_\infty)((1 + (\mathcal{L}\dot{\gamma})^2)^{\frac{n-1}{2}} \tag{5}$$

where η_0 and η_∞ are respectively the zero- and $\inf$-shear-rate viscosities, $\dot{\gamma}$ is the rate of strain modulus and $\mathcal{L}$ is the inverse of $\dot{\gamma}$ in which the power-law region starts – *per unit of time* – and n is the power-law coefficient.

3. NUMERICAL METHOD

The finite element approximation for the governing equations Eq.((1)-(3)) is based on a three-field Galerkin least-square–like formulation, as (Behr *et al.*, 1993) and (Franca and Frey, 1992), in terms of extra-stress, pressure and velocity. Its approximed variational equations runs as: Find the triple $(\boldsymbol{\tau}^h, p^h, \mathbf{u}^h) \in \boldsymbol{\Sigma}^h \times P^h \times \mathbf{V}^h$ such that:

$$\mathcal{B}(\boldsymbol{\tau}^h, p^h, \mathbf{u}^h; \mathbf{S}^h, q^h, \mathbf{v}^h) = F(\mathbf{S}^h, q^h, \mathbf{v}^h) \quad \forall\,(\mathbf{S}^h, q^h, \mathbf{v}^h) \in (\boldsymbol{\Sigma}^h \times P^h \times \mathbf{V}_0^h) \tag{6}$$

where the three-linear form $B(\cdot,\cdot)$ is given by,

$$\begin{aligned}\mathcal{B}(\boldsymbol{\tau}^h, p^h, \mathbf{u}^h; \mathbf{S}^h, q^h, \mathbf{v}^h) = {} & (2\eta(\dot{\gamma}))^{-1}\int_\Omega \boldsymbol{\tau}^h\cdot\mathbf{S}^h d\Omega + (2\eta(\dot{\gamma}))^{-1}\int_\Omega \lambda\check{\boldsymbol{\tau}}^h\cdot\mathbf{S}^h d\Omega - \int_\Omega \mathbf{D}(\mathbf{u})^h\cdot\mathbf{S}^h d\Omega \\ & + \int_\Omega \boldsymbol{\tau}^h\cdot\mathbf{D}(\mathbf{v})^h d\Omega - \int_\Omega p^h div\,\mathbf{v}^h d\Omega + \int_\Omega div\,\mathbf{u}^h q^h d\Omega + \epsilon\int_\Omega p^h q^h d\Omega \\ & + \sum_{K\in\Omega^h}\int_{\Omega^K}(\nabla p^h - div\,\boldsymbol{\tau}^h)\cdot\alpha(\mathbf{x})(-\nabla q^h + div\,\mathbf{S}^h)d\Omega \\ & + 2\,\eta(\dot{\gamma})\beta\int_\Omega (2\,\eta(\dot{\gamma}))^{-1}(\boldsymbol{\tau}^h + (2\eta(\dot{\gamma}))^{-1}\lambda\check{\boldsymbol{\tau}}^h - \mathbf{D}(\mathbf{u})^h)\cdot((2\,\eta(\dot{\gamma}))^{-1}\mathbf{S}^h + (2\,\eta(\dot{\gamma}))^{-1}\lambda\check{\boldsymbol{S}}^h - \mathbf{D}(\mathbf{v})^h)d\Omega\end{aligned} \tag{7}$$

with $\boldsymbol{\Sigma}^h$ the finite stress space, $\mathcal{L}_1(\Omega)\cap\mathcal{C}_1^0(\Omega)^{N\times N}$, P^h is the finite pressure space, $\mathcal{L}^0(\Omega)$, and $\mathbf{V}^h$ is the finite velocity space $\mathcal{H}^1(\Omega)^N$. The functional $F(\cdot)$ is expressed as,

$$\mathcal{F}(\mathbf{S}^h, q^h, \mathbf{v}^h) = \int_\Omega \rho \mathbf{f} \cdot \mathbf{v}^h d\Omega + \int_{\Gamma_h} \mathbf{t}_h \cdot \mathbf{v}^h d\Omega + \sum_{K \in \Omega^h} \int_{\Omega_K} \rho \mathbf{f} \cdot \alpha(\mathbf{x})(\nabla q^h - div \mathbf{S}^h) d\Omega \tag{8}$$

where $\mathbf{t}_n$ is the Cauchy's velocity vector, K is any finite element used in the grid partition of the fluid domain Ω, and $\alpha(\mathbf{x})$ and β and are the stabilized parameters for motion and viscoelastic equations – see the error analysis introduced in (Behr *et al.*, 1993) and (Franca and Frey, 1992).

4. PRELIMINARY RESULTS

In this section are presented preliminary results obtained from the finite element approximation Eq.((6)–(8)) for the flow governing equations Eq.((1)-(3)). Since the material to be investigated is a complex one with elasticity, results focus on the determination of elastic influence, as long with the shear-thinning, on the flow pattern.

The finite variational equations introduced in the previous section, Eq.(6)–(8), are implemented in the Finite Element Computational Code for non-Newtonian fluids (NNFEM) built at Laboratory of Computational, and Applied Fluid Mechanics (LAMAC) of the Department of Mechanical Engineering of Federal University of Rio Grande do Sul.

In the convergence of the highest elastic flows, a zero-order continuation strategy, on the Weissenberg number, is implemented – as well the use of a (numerical) developed solution obtained from the previous quasi-Newton step.

4.1 Geometry and Triangularization

The geometry herein considered is a planar channel subjected to an abrupt contraction of different aspect rations, h_1/h_2 – with h_1 and h_2 denoting the heights upstream and downstream the contraction, respectively. The upstream length is given by $50h_1$ and the downstream one by $30h_1$.

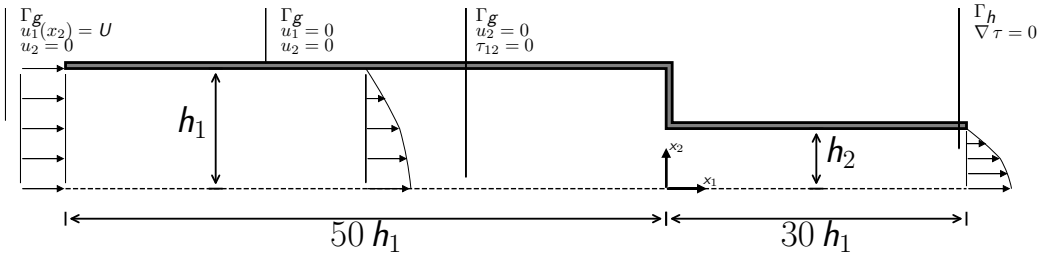

Figure 1: Problem statement for sudden contraction domain. (A detail).

Concerning the boundary conditions, a flat velocity profile at inlet ($u_1 = U; u_2 = 0$), impermeability and no-slip ($u_1 = u_2 = 0$) on walls, parallel velocity and null shear stress ($u_2 = U; \tau_{12} = 0$) at symmetry boundary, and free traction at outlet – see Fig.1 for the problem statement.

After a mesh independence study on the transverse profile of extra stress, the flow domain is partitioned into a combination $5,942$ equal-order bi-linear Lagrangian finite elements, for pressure, extra-stress and velocity – totalizing $36,652$ degrees of freedom.

4.2 Governing Parameters

Considering the following geometric and kinematic and dynamical dimensionless quantities,

$$\begin{aligned} \mathbf{x}^* &= \frac{\mathbf{x}}{h_1} \quad ; \qquad \mathbf{u}^* = \frac{\mathbf{u}}{U} \quad ; \qquad div^* = h_1\, div \quad ; \qquad \nabla^* = h_1 \nabla \quad ; \\ \boldsymbol{\tau}^* &= \frac{\boldsymbol{\tau}\, h_1}{\eta(\dot{\gamma}_c)\, U} \quad ; \qquad p^* = \frac{p\, h_1}{\eta(\dot{\gamma}_c)\, U} \quad ; \qquad \eta(\dot{\gamma})^* = \frac{\eta(\dot{\gamma})}{\eta(\dot{\gamma}_c)} \end{aligned} \tag{9}$$

where U is the characteristic (constant) velocity and h_1 is the flow characteristic length.

Substituting definitions (9) into Eq.(1–5), the dimensionless governing equations are obtained as,

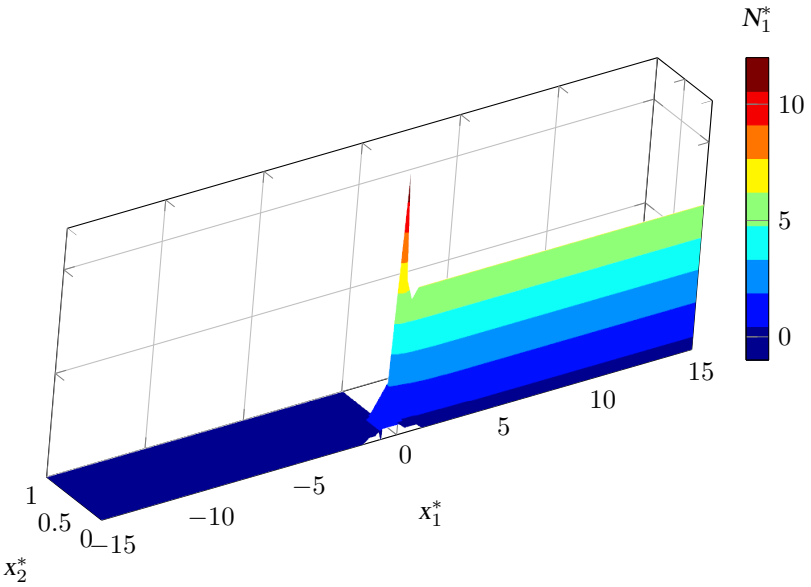

Figure 2: N_1^* elevation plot for $Fr = 1$, $Cu = 0$, $n = 1$ and $Wi = 0.1$. (A detail.)

$$div^*\mathbf{u}^* = \mathbf{0} \quad \text{in } \Omega^* \tag{10}$$

$$\mathbf{0} = -\nabla^* p^* + div^*\boldsymbol{\tau}^* - Fr^{-2}\mathbf{f}^* \quad \text{in } \Omega^* \tag{11}$$

$$\boldsymbol{\tau}^* + Wi\,\check{\boldsymbol{\tau}}^* = \mathbf{D(u)}^* \quad \text{in } \Omega^* \tag{12}$$

$$\check{\boldsymbol{\tau}}^* = (\nabla^*\boldsymbol{\tau}^*)\mathbf{u}^* - (\nabla^*\mathbf{u}^*)^T\boldsymbol{\tau}^* - \boldsymbol{\tau}^*(\nabla^*\mathbf{u}^*) \quad \text{in } \Omega^* \tag{13}$$

$$\eta(\dot{\gamma}^*)^* = \eta_\infty^* + (\eta_0^* - \eta_\infty^*)((1 + (Cu\dot{\gamma}^*)^2)^{\frac{n-1}{2}} \quad \text{in } \Omega^* \tag{14}$$

where Ω^* is the dimensionless flow domain.

From Eq.((10)–(14)), it gives rise the dimensionless parameters that rules the flow investigated, namely, the Froude number Fr, the Weissenberg number and Carreau number, respectively defined as

$$Fr = \frac{U}{\sqrt{|\mathbf{g}|h_1}} \tag{15}$$

$$Wi = \lambda\dot{\gamma}_c \tag{16}$$

$$Cu = \mathcal{F}\dot{\gamma}_c \tag{17}$$

with the characteristic strain rate $\dot{\gamma}_c$ computed as U/h_1.

Fig.(2) show the high N_1^*-value near the small channel wall due to the velocity gradient resultant from the contraction presence. Fig.(3) show the influence of elasticity on the flow pattern. Upstream the contraction, the elastic flow can predict non-null N_1^* even an in a pure shear flow; on the other hand, the same does not occur with the inelastic flow, since the constitutive portion of Cauchy's tensor, for inelastic materials, is deviatoric. Then, in the contraction vicinity, both flows present non-null τ_{11}^*, with the elastic one showing a larger value of τ_{11}^*, due to the relative growth of the elastic term of Eq.(13). It is worth noting that the normal stresses induced by the geometry contraction have no physical meaning for the inelastic flow since this class of fluid is incapable of predicting constitutive elongational stresses. Downstream the contraction, the flow pattern is similar to the one of the large channel, with the only difference that the small channel present larger values of τ_{11}^* – thanks of the larger stress level which the small channel is submitted own the sharp area reduction.

Consider the analytical solution for the fully-developed region of a viscoelastic flow in a planar channel (Behr *et al.*, 2004).

$$\tau_{11}^* = 2\lambda\eta(\dot{\gamma})\left(\frac{-3x_2}{h^2}\right)^2 \tag{18}$$

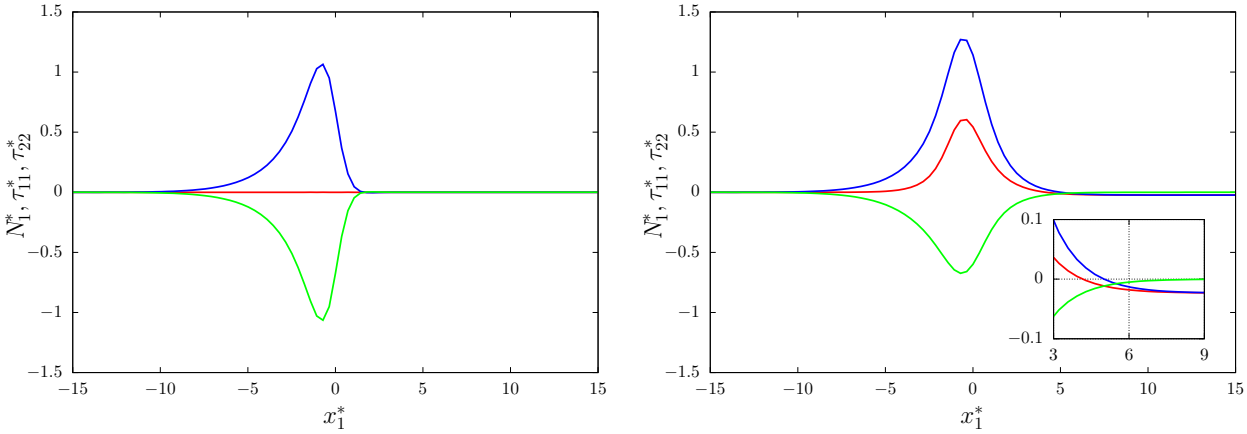

Figure 3: N_1^* (—), $\boldsymbol{\tau}_{11}^*$ (—) and $\boldsymbol{\tau}_{22}^*$ (—) –transverse profile, in fully-developed flows regions, for $Fr = 1$, $Cu = 0$ and $n = 1$ and $Wi = 0.1$: (a) at $x_1^* = -15$ (large channel); (b) at $x_1^* = +15$ (small channel).

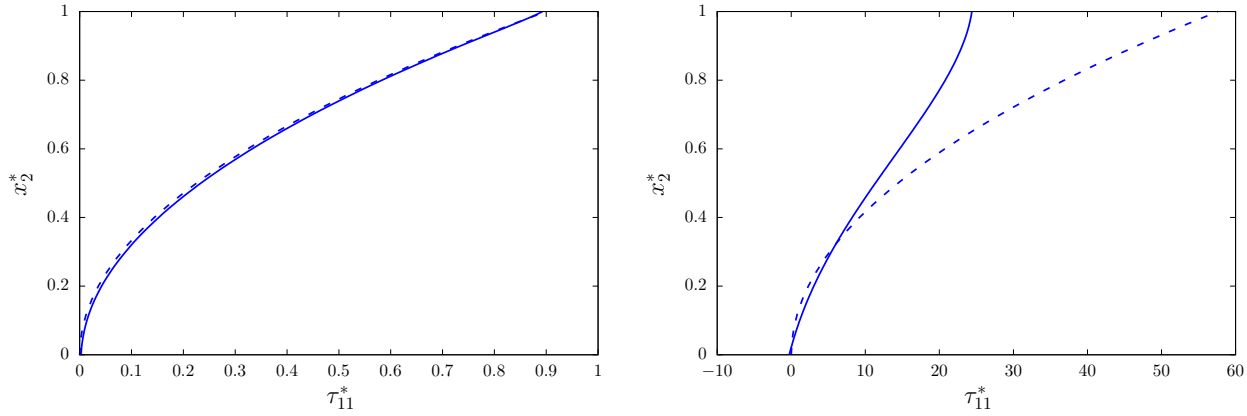

Figure 4: Numerical (—) and analytical (- - -) τ_{11}^*–transverse profile, in fully-developed regions, for $Fr = 1$, $Cu = 0$ and $n = 1$ and $Wi = 0.1$: (a) at $x_1^* = -15$ (large channel); (b) at $x_1^* = +15$ (small channel).

From Fig.(4), it is noticed a fine agreement between our computations and the analytical solution. In Fig.(4a), our computations were able to rebuild the stress analytical even with the flow experiencing a severe inflow due to the imposition of flat stress profile at the inlet. In Fig.(4b), it is noticed a partial agreement with the analytical, with our numerical solution seeming to be over-diffusive. It should take into account that the flow again experiences another tough inflow due to to the high elasticity levels present in the vicinity of contraction plane.

5. ACKNOWLEDGEMENTS

The Authors would like to thank to CNPq and CAPES for financial support.

6. CONCLUSIONS

The current work used a three-field Galerkin least-squares–like method, in terms of extra stress, pressure, and velocity, for approximating inertialess flows of White-Metzner materials through a 4:1 sudden contraction. In preliminary results, it was only considered the elasticity influence on the flow pattern. Then, the impact of the shear-thinning of polymeric viscosity and the variation of aspect ration of contraction are also investigated. The Weissenberg number increase altered the flow pattern profoundly in the vicinity of contraction plane. Results are shown to be physically meaning and in accordance with the viscoelastic literature.

7. REFERENCES

Alves, M.A., Oliveira, P.J. and Pinho, F.T., 2004. "On the effect of contraction ratio in viscoelastic flow through abrupt contractions". *Journal of non-newtonian fluid mechanics*, Vol. 122, No. 1-3, pp. 117–130.

Behr, M., Arora, D. and Pasquali, M., 2004. "Stabilized finite element methods of gls type for oldroyd-b viscoelastic fluid". *European Congress on Computational Methods in Applied Sciences and Engineering ECCOMAS*, pp. 24–28.

Behr, M.A., Franca, L.P. and Tezduyar, T.E., 1993. "Stabilized finite element methods for the velocity-pressure-stress formulation of incompressible flows". *Computer Methods in Applied Mechanics and Engineering*, Vol. 104, No. 1, pp. 31–48.

Crochet, M. and Bezy, M., 1979. "Numerical solution for the flow of viscoelastic fluids". *Journal of Non-Newtonian fluid mechanics*, Vol. 5, pp. 201–218.

Cruz, F., Poole, R., Afonso, A., Pinho, F., Oliveira, P. and Alves, M., 2014. "A new viscoelastic benchmark flow: Stationary bifurcation in a cross-slot". *Journal of Non-Newtonian Fluid Mechanics*, Vol. 214, pp. 57–68.

Franca, L.P. and Frey, S.L., 1992. "Stabilized finite element methods: Ii. the incompressible navier-stokes equations". *Computer Methods in Applied Mechanics and Engineering*, Vol. 99, No. 2-3, pp. 209–233.

Frey, S., Fonseca, C., Zinani, F. and Naccache, M.F., 2010. "Galerkin least-squares approximations for upper-convected maxwell fluid flows". *Mechanics Research Communications*, Vol. 37, No. 7, pp. 666–671.

Oliveira, P.J. and Pinho, F.T.d., 1999. "Plane contraction flows of upper convected maxwell and phan-thien–tanner fluids as predicted by a finite-volume method". *Journal of Non-Newtonian Fluid Mechanics*, Vol. 88, No. 1-2, pp. 63–88.

Tomé, M.F., de Araujo, M.S.B., Alves, M.A. and Pinho, F., 2008. "Numerical simulation of viscoelastic flows using integral constitutive equations: A finite difference approach". *Journal of Computational Physics*, Vol. 227, No. 8, pp. 4207–4243.

Viriyayuthakorn, M. and Caswell, B., 1980. "Finite element simulation of viscoelastic flow". *Journal of Non-Newtonian Fluid Mechanics*, Vol. 6, No. 3-4, pp. 245–267.

8. RESPONSIBILITY NOTICE

The authors are the only responsible for the printed material included in this paper.